Computers & Fluids 45 (2011) 77–83

Contents lists available at ScienceDirect

Computers & Fluids

journal homepage: www.elsevier.com/locate/compfluid

Parallel Domain-decomposed Taiwan Multi-scale Community Ocean Model (PD-TIMCOM)

Yu-heng Tseng *, Mu-hua Chien

Department of Atmospheric Sciences, National Taiwan University, Taipei, Taiwan

ARTICLE INFO

Article history:
Received 30 September 2010
Received in revised form 14 February 2011
Accepted 15 February 2011
Available online 13 March 2011

Keywords:
Ocean General Circulation Model (OGCM),
Domain-decomposition
Error Vector Propagating (EVP)

ABSTRACT

The Parallel Domain-decomposed Taiwan Multi-scale Community Ocean Model (PD-TIMCOM) was developed to provide a flexible and efficient community ocean model for simulating a variety of idealized and real ocean flows over a wide range of scales and boundary conditions. The model is particularly targeted at resolving multi-scale dynamics in the ocean environment, ranging from small scale turbulence to the global circulation gyres. The novel parallel algorithm improves the efficiency of the Error Vector Propagating (EVP) method, a simple direct solver for the typical pressure Poisson equations in the PD-TIMCOM. The new approach is ideal for multiple processes and takes advantage of parallel domain-decomposition, which can significantly reduce the operational counts and computational costs simultaneously. The speed-up is proportional to the number of domains, thus making the PD-TIMCOM a practical eddy-resolving global ocean model for climate projection. We illustrate the parallel performance based on the 1/4° global adaptation of PD-TIMCOM. Our results show accurate meso-scale variability, the reasonable separation of several western boundary currents from the coast, and the appropriate watermass distribution in the global ocean. Consistent with satellite altimetry, the results also show clear mean fronts in the Kuroshio Extension and extensive Kuroshio–Oyashio interaction. This leads to a quasi-equilibrium eddy field associated with three meandering jets in the Kuroshio Extension and Gulf Stream.

1. Introduction

Ocean General Circulation Models (OGCMs) play an important role in the study of ocean circulation, climate systems, and their variations over recent decades. The multi-scale (either spatial or temporal) dynamics in the ocean complicate the accurate representation of the ocean status in the model simulation, ranging from small-scale processes to large scale general circulation [1]. Usually, the small-scale processes are parameterized because resolving all the dynamics within a broad range of scales at the same time is almost impossible.

The successive progress of computational power in recent decades has made it possible to perform high-resolution modelling that can handle multi-scale dynamics. Eddy-resolving OGCMs will become ever more feasible in the near future. In this paper, we introduce a Parallel Domain-decomposed version of the Taiwan Multi-Scale Community Ocean Model (PD-TIMCOM). The PD-TIMCOM can provide a flexible and efficient community ocean model for simulating a variety of idealized and real ocean flows over a wide range of scales and boundary conditions. In particular, the global adaptation of PD-TIMCOM facilitates the global ocean climate study. The success of a high-resolution OGCM requires an effective pressure Poisson solver. Thus, this novel parallel algorithm improves the efficiency of the Error Vector Propagating (EVP) method, a simple direct solver for typical pressure Poisson equations. It has been shown that the EVP method is ideal for parallel domain-decomposition [2].

As the first step toward a global eddy-resolving OGCM for the study of climate variability, we address the recent advances in modelling the general ocean circulation at the eddy-permitting resolution (1/4°) achieved in the framework of the Taiwan Multi-scale Community Ocean Model [3], TIMCOM. The eddy-permitting global ocean circulation model is still worth exploring and enhancing despite the existing higher resolution model because the next generation of fully-coupled climate models will be within the target resolution [4]. Furthermore, this model framework will be used to develop the ultra-fine global ocean model in the next phase. The primary purpose of this study is to describe the general characteristics of the simulation, which may subsequently be built upon for a more detailed analysis. In this paper, we highlight several key features of the model, including its parallel performance, and

* Corresponding author.
E-mail address: yhtseng@as.ntu.edu.tw (Y.-h. Tseng).

0045-7930/$ - see front matter © 2011 Elsevier Ltd. All rights reserved.
doi:10.1016/j.compfluid.2011.02.012

present the results. This guides us toward the future development of the eddy-resolving PD-TIMCOM and the estimation of its computational cost.

2. Global 1/4° PD-TIMCOM configuration

2.1. Model setting

The eddy-permitted global simulation described here is based on the global adaptation of the Taiwan Multi-scale Community Ocean Model using a Mercator grid with a 1/4° longitudinal resolution and linear-exponential stretched grid of 25 layers. It is a hydrostatic, z-level, fourth-order accurate OGCM [3,5,6]. Horizontal momentum, heat and salt material conservation laws and the incompressibility (Boussinesq), hydrostatic and rigid-lid approximations are invoked. Density is defined by an equation of state relating density nonlinearly to temperature, salinity and pressure-depth [5]. Model bathymetry is interpolated from the unfiltered 2-min ETOPO-2 depth data (http://www.ngdc.noaa.gov/mgg/global/relief/ETOPO2/). The vertical resolution is a linear-exponential stretched grid of 25 layers with a thickness of roughly 10 m in the top layer. The model domain covers the entire globe from 72°S to 72°N. The northern boundary is closed and is slowly nudged toward climatology in a sponge layer. Note that the global vertical structure is mostly governed by the hydrostatic approximation and strong stratification, except at high latitudes. The large scale Sverdrup circulation and geostrophic currents dominate so that 25 layers are sufficient to reasonably resolve the vertical structure including the Kuroshio and Gulf Stream. However, if the main interest is the dynamics in the upper and bottom boundary layers, the model requires further vertical resolution and better turbulent parameterization.

The surface wind forcing is obtained from the interpolated monthly Hellerman and Rosenstein winds [7]. The Levitus'94 climatology [8] is used to initialize the model and to determine its surface sources of heat using the non-damping approach described in [9]. Surface salinity is maintained by exchanges of salt with the second layer, ignoring the minor effects of surface fresh water volume sources/sinks. The ocean bottom is insulated and patterned by a nonlinear drag approximation. The subgrid-scale vertical mixing is parameterized by eddy diffusivity (for temperature and salinity) and viscosity (for momentum) using a modified Richardson number dependent formula based on Pacanowski and Philander [10]. More detailed description can be found in [3,5,6,11,12] but not the global adaptation performed in the current study.

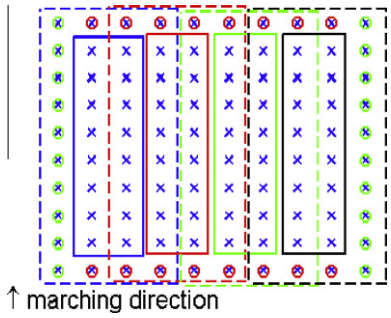

Fig. 1. The parallel SEVP is solved along the latitudinal direction and the decomposed domains composed by computation region with solid lines and ghost zone covered by dashed lines.

Table 1
Platform for parallel performance tests.

Platform	CPU	Total cores	Network
IBM cluster 1350	Intel Woodcrest 3.0 GHz (dual-core x2)	2640	InfiniBand
IBM iData Plex	Intel Nehalem 2.67 GHz (quad-core x2)	3200	InfiniBand
Cray XT5	Opteron 2.4 GHz (quad-core x2)	5312	SeaStar
Cray XT4	Opteron 2.3 GHz (quad-core x2)	38,288	SeaStar2

2.2. Parallel algorithm and the modified SEVP solver based on the parallel domain-decomposition

The novel parallel algorithm improves the efficiency of the Stabilized Error Vector Propagating (SEVP) method, a simple direct solver for the typical pressure Poisson equations in the PD-TIMCOM [2].

$$\frac{\partial^2 u_i}{\partial x_i^2} = \phi \tag{1}$$

where u_i is the required solution along the i direction, ϕ is the forcing function, and the operator $\partial^2/\partial x^2$ is the second order spatial partial derivative.

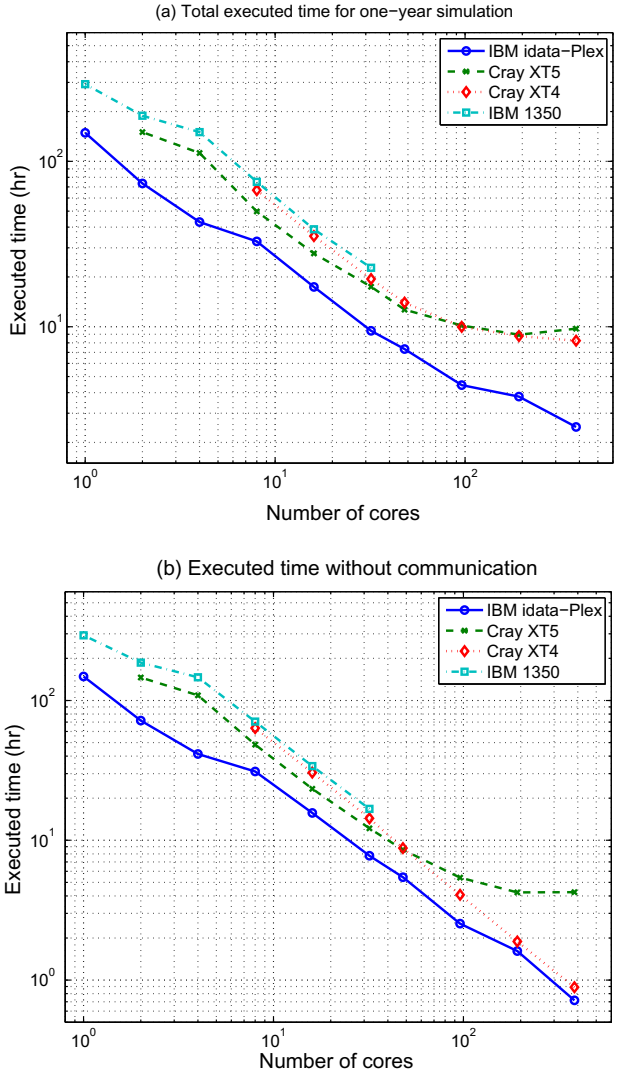

Fig. 2. (a) Total executed time for one-year simulation of PD-TIMCOM for a variety of cores and different platforms. (b) The computation only (communication time excluded) time for a variety of cores and different platforms.

The traditional SEVP solver is already based on the idea of domain-decomposition [2]. The new approach is ideal for multiple computing processers and takes further advantage of parallel domain-decomposition. The layout of our parallel domain-decomposition with the SEVP algorithm is shown in Fig. 1. The whole simulation domain is represented by x while the circle ○ marks the ghost zone boundary. We march the solution along the latitudinal direction so that the domain-decomposition applies in the longitudinal direction [2]. The domain-decomposition also takes advantage of the ghost zone of each domain, which is shown by the rectangular blocks (dashed lines mark the ghost zones and the actual grid points while the solid line covers the actual grid points). The operation count of this algorithm is bounded by $O(n^{3/2})$, where n is the number of horizontal grid points. Solving the same problem with the Multigrid method requires $O(n)$ for each iteration and $O(n\log n)$ iterations to converge, thus the computational cost of the Multigrid method is bounded by $O(n^2\log n)$. This is a significant advantage of the SEVP solver. Furthermore, the parallel Multigrid approach requires $O(n\log n)$ to communicate whereas the parallel SEVP only requires $O(n^{1/2}xN_p)$, where N_p is the number of processors, which is normally much less than n. Therefore, both the operation count and the communication cost of SEVP are much lower than for the multigrid method for a large-scale modelling system such as the eddy-resolving global ocean model. Further discussion and the details of the algorithm can be found in [13].

3. Parallel performance

We next evaluate the performance of the global PD-TIMCOM on several platforms for the sake of portability, including the IBM cluster 1350, IBM iData Plex, Cray XT4 and Cray XT5. The detailed configuration is shown in Table 1. We used up to 384 cores on all platforms except the IBM cluster 1350 for the global simulation, and the total wall-clock time for a 1-year simulation is approximately 11.5 h (Fig. 2a). This indicates that, for such a resolution, the 100-year simulation can be easily completed within 48 days based on the available computational resources.

The computational cost is extremely heavy for the global 1/4° model (size: longitude × latitude × depth = 1442 × 722 × 25) so that the model cannot be run successfully on some platforms when a small number of cores (or a single process) is used, due to the constraints between platforms, software limitations and memory arrangement. We set the speed-up equal to unity for the smallest number of available cores. The overall speed-up is significant mainly because of the specially-designed parallel algorithm and the requirement for less dynamic memory within the cache (Table 2). The parallel algorithm favours the use of a larger number of cores. Fig. 2b shows the total wall-clock time of the numerical computation without the communication part (communication time excluded) for a variety of cores and different platforms. The total time decreases with an increasing number of cores, which is mainly due to the significant reduction in computation. The speed-up is quite linear until 96 cores are used for all platforms. Note that the communication cost can be ignored when comparing the computation cost for a small number of cores, but becomes significant with an increasing number of processors. More discussion of the parallel performance and the new parallel EVP solver can be found in [13]. It is also clear that the SEVP solver is key to reducing the computational cost. Further improvements and optimization are ongoing.

4. Model results

4.1. General features

We describe some preliminary model results to demonstrate the capability of the model. Fig. 3 shows the global 10-year averaged sea surface height and upper 50 m velocity vector for the simulation years 41–50. It is clear that most of the current

Table 2
Overall speed-up.

Comput. cores	1	2	4	8	16	32	48	96	192	384
IBM cluster 1350	1	1.55	1.95	3.89	7.73	12.88				
IBM iDATA Plex	1	2.02	3.46	4.53	8.54	15.73	20.27	33.47	39.30	59.93
Cray XT 5		1	1.34	3.02	5.41	8.60	11.83	14.76	16.77	15.41
Cray XT 4				1	1.90	3.44	4.78	6.71	7.62	8.13

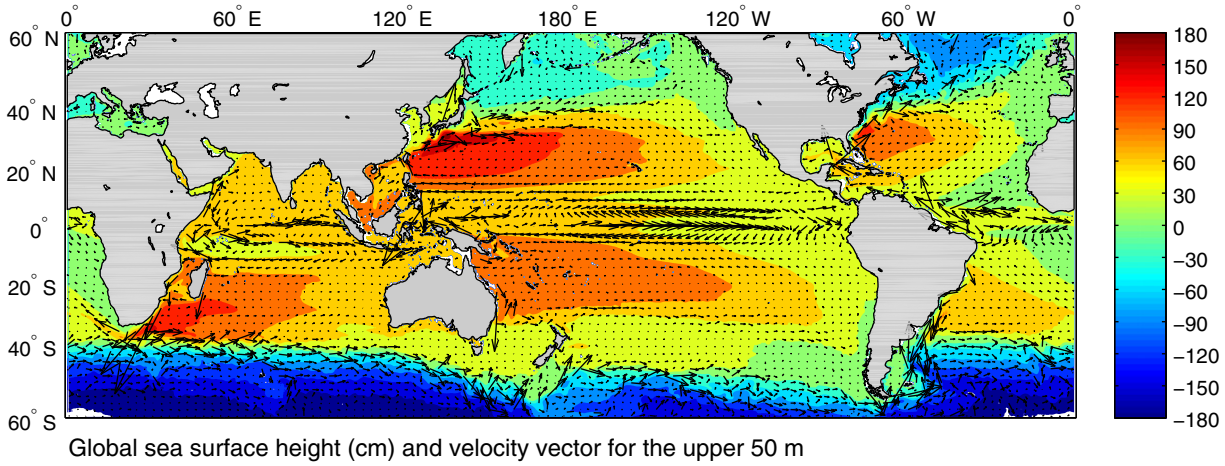

Fig. 3. 10-Year averaged global equivalent sea surface height (cm) and upper 50 m velocity vector at simulation year 41–50.

systems develop reasonably well with time. In particularly, the major western boundary current systems evolve into their quasi-equilibrium states. Fig. 4a presents the complex Kuroshio–Oyashio fronts in the Northwest Pacific from the five-day mean upper 50 m velocity vector and speed fields (day 130–135, year 40). Consistent with satellite altimetry, our results show clear fronts in the Kuroshio Extension and extensive Kuroshio–Oyashio interaction. This leads to a quasi-equilibrium eddy field associated with three meandering jets in the Kuroshio Extension. Particularly, the Kuroshio southeast of Japan shows the typical large meandering path. Multiple fronts are also presented, indicating the unstable dynamics in this region. Fig. 4b shows the simulated 5-day mean Gulf Stream upper 50 m velocity vector and speed on day 130–135, year 40. In the North Atlantic, the modelled Gulf Stream shows quite reasonable separation and the pinch-off eddies when comparing with the observation.

4.2. Kuroshio

Fig. 5a shows the equivalent SSH distribution in the Kuroshio/Kuroshio Extension region averaged over 10 years for years 41–50. The simulated Kuroshio flows along the south coast of Japan and leaves the coast into the Pacific. The location and meandering path of the main stream along the Ryukyu island chain and southern Japan agree well with observations. The Kuroshio separation near 36°N is also consistent with observations of two associated standing eddies [14]. Note that there is no model tuning and the global resolution is 1/4°. The separated jet bifurcations are even clearer in the Kuroshio Extension region, where the separated current totally escapes from the kinematic constraints of shelfslope bathymetry. Another clear subpolar front develops near the coast of Japan at 38–39°N (Fig. 4a). A Kuroshio/Oyashio mixed water region lies between these two fronts.

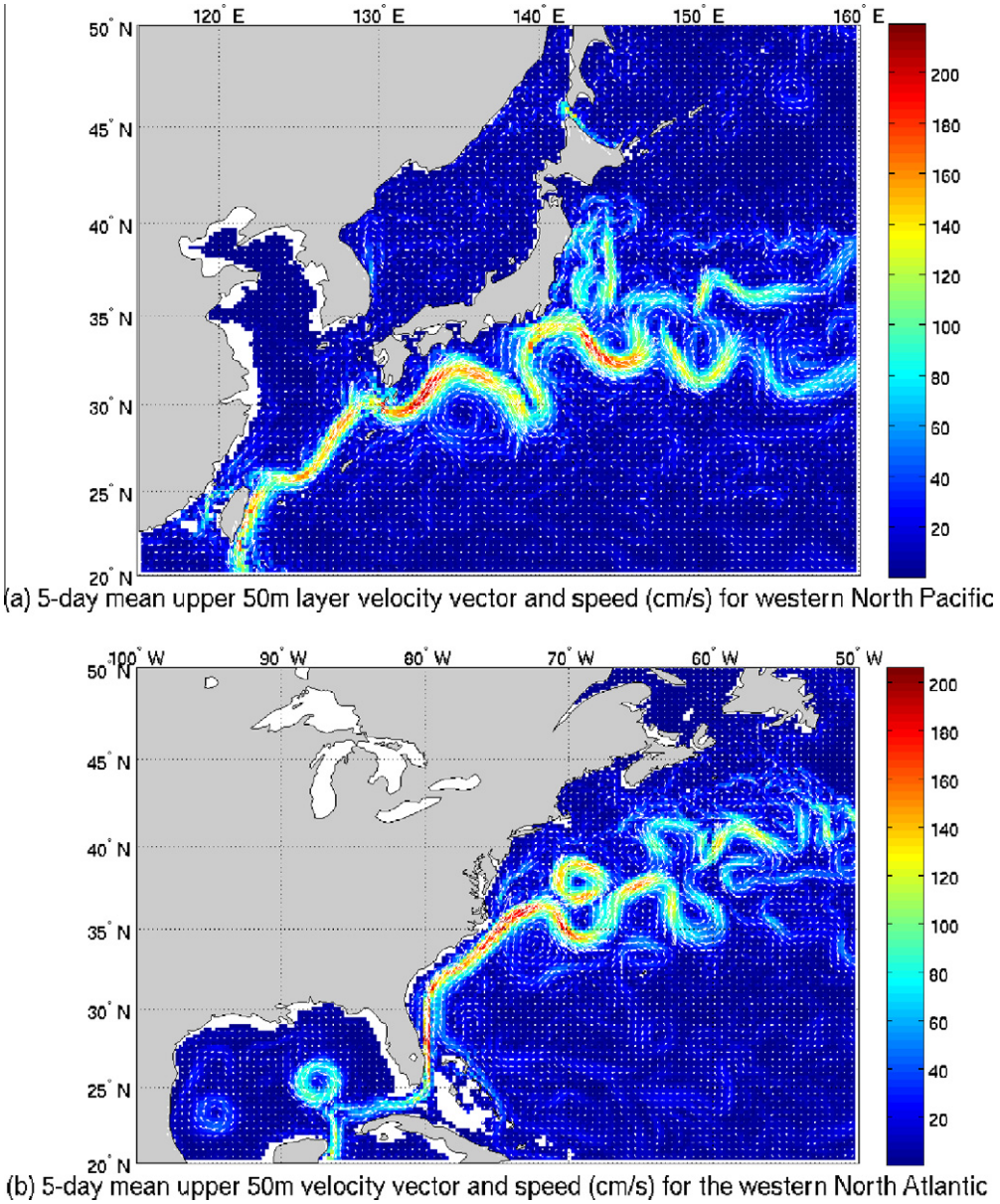

Fig. 4. (a) Modelled 5-day mean upper 50 m velocity vector and speed for the western North Pacific at day 130–135 year 40. (b) Modelled five-day mean upper 50 m velocity vector and speed for the western North Atlantic at day 130–135 year 40.

The comparison of the time averaged (year 41–50) second moment (standard deviation of the equivalent sea surface height) in the Kuroshio between the model and the satellite altimetry is shown in Fig. 6a and b. The observed sea level variation is derived from the weekly gridded altimetry data at 1/3° resolution [15] for the period 1993–2001. It is based on delayed-mode data from the TOPEX/Poseidon, Jason 1, ERS1/2 and ENVISAT satellite altimeter missions processed by the Space Oceanography Division of Collection Localisation Satellites located in Toulouse, France. The model shows a relatively realistic eastward extension. However, the strength seems slightly weaker in the model results because of the eddy-permitting resolution.

4.3. Gulf Stream

Fig. 5b shows the modelled 10-year averaged (years 41–50) sea surface height (in cm) in the North Atlantic. To evaluate the mean path, the mean SSH is overlaid with the 15-year mean Gulf Stream IR northwall pathway $\pm 1\sigma$ (standard deviation) by Cornillon and Sirkes (unpublished 2010). This frontal pathway has a 0.1° longitudinal resolution and lies along the northern edge of the Gulf Stream. The mean path of the Gulf Stream shows a clear separation at Cape Hatteras. This is associated with an elongated anticyclonic recirculation south of the Gulf Stream and a cyclonic recirculation to the north. The modelled frontal pathway agrees well with long-term observations. The cyclonic recirculation indicates the presence of cold slope waters on the Grand Banks, and a crossing of the 40°N line near 300°E. Beyond this point, the path of the North Atlantic Current (NAC) is characterized by a clearly marked Mann Eddy around 42.5°N, 315°E, which is a large permanent anticyclonic eddy located adjacent to the NAC at this latitude, and a North West Corner at 50°N, 40°W [4]. Thus, the path of modelled NAC is consistent with the observation north of 50°N, and follows the topography.

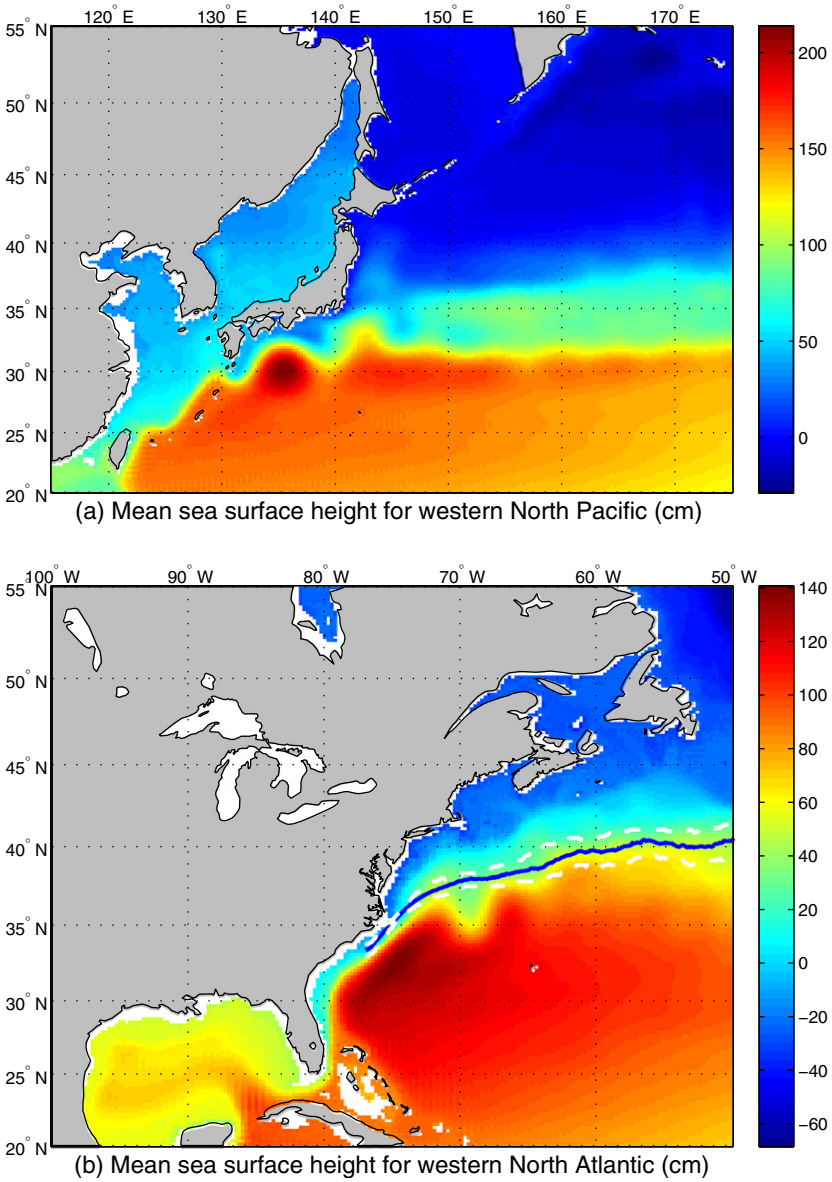

Fig. 5. The modelled 10-year averaged (year 41–50) equivalent sea surface height (in cm) for the North Pacific (a) and North Atlantic (b), respectively. On (b), the mean Gulf Stream IR northwall pathway $\pm 1\sigma$ (standard deviation) by Cornillon and Sirkes (unpublished) is superimposed. This frontal pathway has 0.1° longitudinal resolution and lies along the northern edge of the Gulf Stream.

Thus, the eddy-permitting 1/4° global model simulates Gulf Stream separation and path reasonably well. Warm and cold core eddies often pinch off as the northward/southward Gulf Stream meanders. The cyclonic (anticyclonic) recirculation gyres occurring north (south) of the Gulf Stream in associated with the cold/warm core eddies. A strong Gulf Stream penetrates into the eastern Grand Banks region. Fig. 6c and d compares the time averaged (year 41–50) second moment (standard deviation of the equivalent sea surface height) in the North Atlantic based on model results with the second moment based on satellite altimetry from 1993–2001 [15]. Both mean time and standard deviation of the modelled Gulf Stream are close to observations, in spite of the eddy-permitting 1/4° resolution. Note that the second moment relies on how well the deformation radii are resolved in the model. Comparisons between models must be moderated by taking the differences in their resolution into account. The spatial pattern of distribution is more important for an eddy-permitting model, which reflects the positions of the main currents and eddy pathways, rather than the magnitude directly. The model result is quite consistent with observations, in particular, along the path of the Gulf Stream and the NAC.

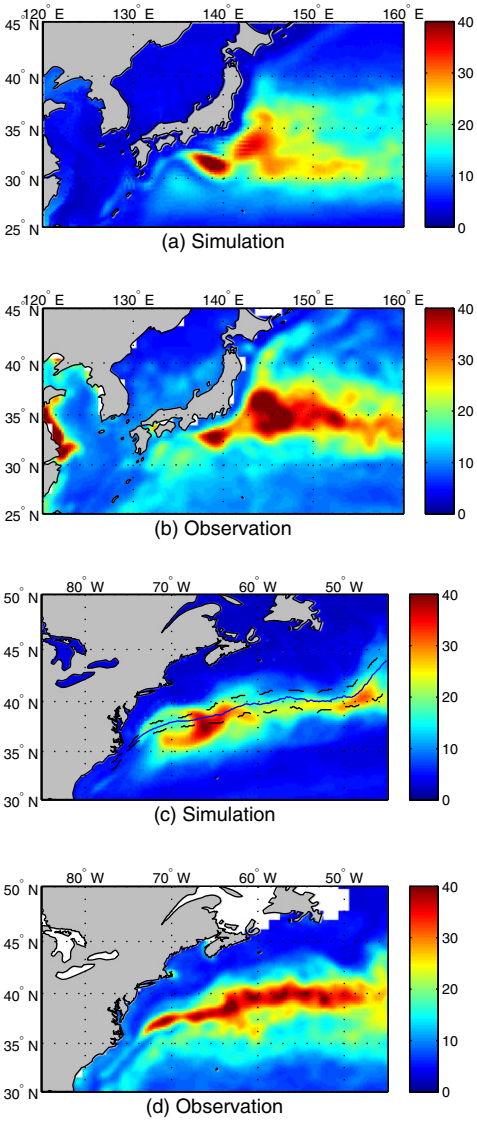

Fig. 6. The modelled (a) and observed (b) 10-year standard deviation (year 41–50) of equivalent sea surface height (in cm) in the Kuroshio. The observed standard deviation (in cm) of sea level is based on weekly gridded altimeter data for the period 1993–2001 [14]. The modelled (c) and observed (d) 10-year standard deviation (year 41–50) of equivalent sea surface height (in cm) in the North Atlantic. The mean Gulf Stream IR northwall pathway ±1σ (standard deviation) by Cornillon and Sirkes (unpublished) is superimposed. See text for the explanation. Bottom: The observed standard deviation (in cm) of sea level based on weekly gridded altimeter data for the period 1993–2001 [14].

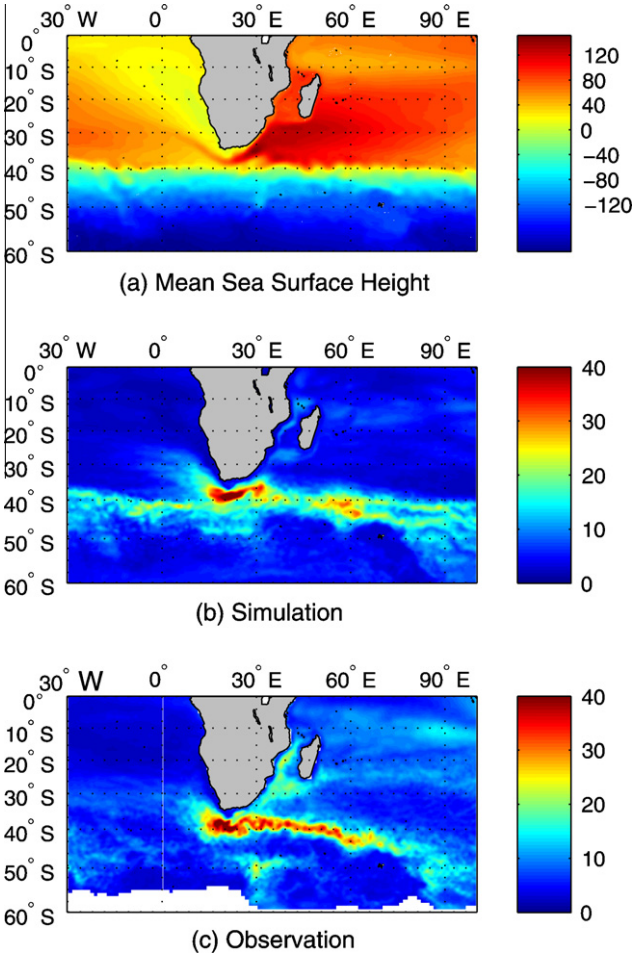

Fig. 7. (a) The modelled 10-year averaged (year 41–50) sea surface height (in cm) in the Agulhas Current and Mozambique Channel region. The modelled (a) and observed (b) 10-year standard deviation (year 41–50) of equivalent sea surface height (in cm) in the Agulhas Current. The observed standard deviation (in cm) of sea level is based on weekly gridded altimeter data for the period 1993–2001 [14].

4.4. Agulhas Current and Mozambique Channel region

Fig. 7a shows the time average equivalent SSH distribution for years 41–50 in the region covering the Agulhas Current and Mozambique Channel. This clearly shows retroflection eddies shed by the Agulhas Current, which appear to be modulated by warm core eddies in the Mozambique Channel. The latter appear to be a result of positive vorticity generation by bottom drag acting along a sloping bottom on the northern branch of the South Equatorial Current, which splits around the island of Madagascar [4]. The southern branch feeds the core of the Agulhas Current and receives positive vorticity from the earth's vorticity advection. The combined effect leads to a series of intense warm core rings due to the shear instability. The ring generation is very regular in time; rings shed from the retroflection are quite large in size and follow similar pathways when propagating across the South Atlantic Ocean.

The ring generation process can be further identified in the time average second moment (standard deviation of the equivalent sea surface height) based on the model results and satellite altimetry (Fig. 7b and c). The reasonable agreement with observations shows that the Mozambique Channel eddies have been accurately modelled.

5. Conclusion

In this paper, we presented the successful development of PD-TIMCOM. The new parallel SEVP solver shows ideal scalability for the large-scale global ocean model, and even favours the extremely high resolution model development with an appropriate increase in the computational cores. The results display clear Kuroshio fronts and accurate Gulf Stream separation, which are comparable with or even better than the typical results of other eddy-resolving models. The Agulhas Current shows significant ring generation due to the shear instability, which may propagate across the South Atlantic Ocean. The computational performance is also superior. One year of model simulation requires only approximately 11.5 h of CPU computation on a 32 core Cray XT5 system. In particular, our global model implementation is ideal for the BlueGene/L type system, which has well-documented high power efficiency and excellent scalability because no global array is required. This leads to the easy extension to the ultra-fine eddy-resolving global model system in the near future.

Acknowledgements

The authors acknowledge the support from National Science Council, Taiwan (Grant number 992628M002010) and computing resource of National Center for High-Performance Computing, Taiwan and NERSC, USA. Statistical observation data provided from Dr. Jim Richman and Prof. Keith Thompson are also appreciated.

References

[1] Griffies SM et al. Formulation of an ocean model for global climate simulations. Ocean Sci 2005;1:45–79.
[2] Roache PJ. Elliptic marching methods and domain decomposition. Boca Raton (Fla): CRC Press Inc.; 1995. 190pp..
[3] Tseng YH, Shen ML, Jan S, Dietrich DE, Chiang CP. Validation of the Kuroshio current system in the dual-domain Pacific ocean model framework. Prog Oceanogr, in press.
[4] Barnier B, Madec G, Penduff T, Molines J-M, Treguier A-M, Le Sommer, et al. Impact of partial steps and momentum advection schemes in a global circulation model at eddy permitting resolution. Ocean Dyn 2006;56:543–67.
[5] Tseng YH, Ferziger JH. Regional circulation of the Monterey Bay region – hydrostatic versus non-hydrostatic modeling. J Geophys Res Ocean 2005;110:C09015. doi:10.1029/2003JC00215.
[6] Shen M-L, Tseng YH, Jan S. The formation and dynamics of the cold-dome off northeastern Taiwan. J Mar Syst 2011;86:10–27.
[7] Hellerman S, Rosenstein M. Normal monthly wind stress over the world ocean with error estimates. J Phys Oceanogr 1983;13:1093–104.
[8] Levitus S, Boyer T. World ocean atlas 1994. Temperature, vol. 4; 1994 [150 pp., NOAA Atlas NESDIS 4].
[9] Dietrich DE, Haney RL, Fernandez V, Josey S, Tintore J. Air–sea fluxes based on observed annual cycle surface climatology and ocean model internal dynamics: a non-damping zero-phase-lag approach applied to the Mediterranean Sea. J Mar Syst 2004;52:145–65. doi:10.1016/j.jmarsys.2004.01.006.
[10] Pacanowski RC, Philander SGH. Parameterization of vertical mixing in numerical models of tropical oceans. J Phys Oceanogr 1981;30:1069–82.
[11] Dietrich DE, Tseng YH, Medina R, Liste M, Olabarriet M, Piacsek S, et al. Accurate Mediterranean overflow water (MOW) simulation using a coupled multiple-grid Mediterranean Sea/North Atlantic Ocean model on a PC. J Geophys Res Ocean 2008;113:C07027. doi:10.1029/2006JC00391.
[12] Tseng YH, Jan S, Dietrich DE, Lin I-I, Chang YT, Tang TY. Modeled oceanic response and sea surface cooling to typhoon Kai-Tak. Terr Atmos Ocean Sci 2010;21:85–98.
[13] Chien MH, Tseng YH. An efficient parallel domain-decomposed marching solver for pressure equation in the Ocean General Circulation Model. In: The 17th computational fluid dynamics conference in Taiwan, July 29–31, Longtan, Taiwan; 2010.
[14] Qiu B, Chen S, Hacker P, Hogg N, Jayne S, Sasaki H. The Kuroshio Extension northern recirculation gyre: profiling float measurements and forcing mechanism. J Phys Oceanogr 2008;38:1764–79.
[15] Thompson KR, Demirov E. Skewness of sea level variability of the world's oceans. J Geophys Res Ocean 2006;111:C05005. doi:10.1029/2004JC002839.